2021

Impulsive Volcanic Plumes Generate Volcanic Lightning and Vent Discharges: A Statistical Analysis of Sakurajima Volcano in 2015

Cassandra M. Smith
University of South Florida

Damien Gaudin
University of Munich

Alexa R. Van Eaton
U.S. Geological Survey

Sonja A. Behnke
Los Alamos National Laboratory

Steven Reader
University of South Florida, sreader@usf.edu

See next page for additional authors

Geophysical Research Letters

RESEARCH LETTER
10.1029/2020GL092323

Key Points:

- Eruptive activity from Sakurajima volcano, 2015 showed that volcanic lightning was a clear indicator of an ash-bearing volcanic eruption cloud
- Vent discharges were linked to impulsive, high-velocity plumes, whereas lightning flashes were linked to plumes with high volume flux
- We infer that the charging for vent discharges is tied to the source explosion while volcanic lightning is governed by volcanic plume processes

Supporting Information:

Supporting Information may be found in the online version of this article.

Correspondence to:

C. M. Smith,
smithcm09@gmail.com

Citation:

Smith, C. M., Gaudin, D., Van Eaton, A. R., Behnke, S. A., Reader, S., Thomas, R. J., et al. (2021). Impulsive volcanic plumes generate volcanic lightning and vent discharges: A statistical analysis of Sakurajima volcano in 2015. *Geophysical Research Letters*, *48*, e2020GL092323. https://doi.org/10.1029/2020GL092323

Received 28 DEC 2020
Accepted 9 MAY 2021

Impulsive Volcanic Plumes Generate Volcanic Lightning and Vent Discharges: A Statistical Analysis of Sakurajima Volcano in 2015

Cassandra M. Smith[1,5], Damien Gaudin[2], Alexa R. Van Eaton[3], Sonja A. Behnke[4], Steven Reader[5], Ronald J. Thomas[6], Harald Edens[6], Stephen R. McNutt[5], and Corrado Cimarelli[3]

[1]Alaska Volcano Observatory, Anchorage, AK, USA, [2]Ludwig Maximilian University of Munich, Munich, Germany, [3]U.S. Geological Survey, Cascades Volcano Observatory, Vancouver, WA, USA, [4]Los Alamos National Laboratory, Los Alamos, NM, USA, [5]University of South Florida, Tampa, FL, USA, [6]New Mexico Institute of Mining and Technology, Socorro, NM, USA

Abstract The origin of electrical activity accompanying volcanic ash plumes is an area of heightened interest in volcanology. However, it is unclear how intense an eruption needs to be to produce lightning flashes as opposed to "vent discharges," which represent the smallest scale of electrical activity. This study targets 97 carefully monitored plumes <3 km high from Sakurajima volcano in Japan, from June 1 to 7, 2015. We use multiparametric measurements from sensors including a nine-station lightning mapping array and an infrared camera to characterize plume ascent. Findings demonstrate that the impulsive, high velocity plumes (>55 m/s) were most likely to create vent discharges, whereas lightning flashes occurred in plumes with high volume flux. We identified conditions where volcanic lightning occurred without detectable vent discharges, highlighting their independent source mechanisms. Our results imply that plume dynamics govern the charging for volcanic lightning, while the characteristics of the source explosion control vent discharges.

Plain Language Summary There are different types of electrical activity that occur within volcanic ash plumes. One well-known type is volcanic lightning, which creates the familiar flashes of visible light. Another, lesser-known type is called "vent discharges," which are tiny and invisible but create a peculiar signal known as continual radio frequency. Vent discharges are important because they sometimes occur very early in an eruption and may provide a way to give early warning of volcanic hazards. For this study, we used a specialized instrument called a lightning mapping array to measure the electrical activity during small eruptions at Sakurajima volcano. We explored when lightning flashes and vent discharges occurred during 97 different explosions. First, we found that the two types did not always happen in the same explosion, showing they are caused by different processes. Second, we found that vent discharges were more likely to occur when the explosive plume rose quickly, possibly because rock breakup and particles rubbing together create a static charge close to the vent. In contrast, lightning flashes occurred when the plume had high volume flux. These findings give clues about how to link electrical signals to eruptive processes for volcano monitoring.

1. Introduction

Explosive ash plumes at a variety of volcanoes, including Sakurajima volcano in Japan, often result in dazzling displays of volcanic lightning (Aizawa et al., 2010, 2016; Behnke et al., 2018; Cimarelli et al., 2016; Smith, Van Eaton, Charbonnier, et al., 2018). Volcanic lightning occurs during explosive, ash-rich eruptions (where magma fracturing and ash particle interactions generate charge through fractoemission and triboelectrification, respectively), indicating the presence of hazardous ash in the atmosphere (Gaudin & Cimarelli, 2019; Mather & Harrison, 2006; McNutt & Thomas, 2015; Méndez Harper & Dufek, 2016; Smith, Van Eaton, Said, & Holzworth, 2018; Van Eaton et al., 2020). Ice generation in high altitude plumes also contributes to charge generation in a process believed to be analogous with thunderstorm charging (e.g., Calbuco, Van Eaton et al., 2016; Bogoslof, Van Eaton et al., 2020; Anak Krakatau, Prata et al., 2020, meteorological thunderstorms, Williams & McNutt, 2005; Carey et al., 2019). Yet, at the lower plume heights common at

Sakurajima (<5 km), plume temperatures remain too warm for ice formation (Cimarelli et al., 2016), allowing us to focus on plume dynamics and silicate charging for this study. Thunderstorm flash rates have been positively connected to updraft volume changes of meteorological clouds, but plume volume has not been previously analyzed for correlations with volcanic lightning studies (Calhoun et al., 2013; Deierling & Petersen, 2008; Deierling et al., 2008; Schultz et al., 2017).

It is well established that high-intensity eruptions produce globally detected volcanic lightning (Mather & Harrison, 2006; McNutt & Williams, 2010). Several studies have addressed thresholds for volcanic lightning production detected by regional or global networks that use very low frequency (VLF) signals (Arason et al., 2013; McNutt et al., 2013; Van Eaton et al., 2020). Magnetotelluric studies are able to record smaller volcanic lightning flashes than regional or global VLF systems and have been used at Sakurajima volcano in coordination with high-speed optical video recordings to record weak cloud-to-ground and in-cloud lightning flashes that occurred near the vent (Aizawa et al., 2016). Magnetotelluric measurements have also been used with a combination of normal-speed and high-speed camera acquisition and infrasound signals to further investigate these small flashes in the near-vent region of Sakurajima (Cimarelli et al., 2016). This study indicated that, similarly to earlier studies at Redoubt Volcano (Behnke et al., 2013), there are positive correlations between the infrasound peak pressure and electrical activity, as well as between the plume height and electrical activity (using optical data at Sakurajima and very high frequency (VHF) lightning mapping data at Redoubt). These relationships between electrical activity and plume height indicate the possibility of plume dynamics being an important factor for volcanic lightning development.

Unfortunately, these long-range antennas and video and magnetotelluric sensors that have been previously used in field campaigns at Sakurajima cannot detect the smallest scales of electrical activity (Behnke & McNutt, 2014). There is a corresponding gap in our understanding of how intense an eruption needs to be to generate the smallest scale of electrical discharges. Of particular interest is the phenomenon known as vent discharges, which manifest in radio frequency measurements as continual radio frequency (CRF) impulses due to their repetition rates over long time scales (Behnke et al., 2018). Vent discharges and subsequent CRF signals are not optically visible and have thus far only been recorded with lightning mapping arrays using VHF sensors. In this paper we will use the terms vent discharges and CRF interchangeably. CRF detection may provide valuable early warning of explosive activity because the signals can develop immediately at the start of the eruption (Behnke et al., 2013, 2018; Behnke & McNutt, 2014). However, there are some eruptions that fail to produce any detectable lightning or CRF signals, which leads to some fundamental questions. How large does an explosive eruption need to be to create volcanic lightning, CRF, or both? And what eruptive processes govern their development?

To investigate these issues, we focus on a series of carefully monitored, small-scale explosions (plume heights < ~3 km, durations < ~5 min) from Sakurajima volcano in Japan, from June 1 to 7, 2015. The volcano was exceptionally active during this period, generating >100 plumes from Showa Crater, with plume heights ranging from a few hundred meters to ~3 km above the vent. There were varying ascent rates, ash contents, and production of vent discharges and lightning (Smith, Van Eaton, Charbonnier, et al., 2018). We recorded the electrical activity using a nine-station lightning mapping array, two broadband seismometers, six infrasound sensors, a thermal infrared camera (30 fps), and a low light camera (30 fps). We analyzed plume ascent characteristics from the infrared videos (including initial jet velocity, peak jet velocity, peak volume flux, and cumulative plume volume—Table S1). We also include the seismic and infrasound signals from this time period, as reported by Smith et al. (2020), and develop a multi-variable linear regression model between the eruptive and electrical observations. Ultimately, we show that CRF and volcanic lightning are most highly correlated to different plume parameters and that CRF requires stronger/larger eruptions (as defined by higher infrasound energies and larger volumes) to occur.

2. Methods

2.1. Quantifying Eruption Dynamics

The video data used in this study were acquired with a FLIR SC600 thermal infrared camera and secondary footage by a Watec low-light camera, both located at the Kurokami branch of the Sakurajima volcano Observatory (SVO), on the eastern flank of Sakurajima volcano (Figure S1). The image size on the thermal

camera is 640 × 480 pixels. Using a distance from camera to vent of 3,683 m (determined by laser telemetry) and an instantaneous field of view of 6.5×10^{-4} radians, and we calculated the side of each square pixel to be 2.394 m. The Watec camera used an auto-iris lens with a wider field of view than the infrared camera and recorded continuous black and white videos (30 fps).

The infrared camera data were analyzed using "Rise Diagrams" (as first described in Gaudin, Taddeucci, Scarlato, delBello, et al., 2017; Gaudin, Taddeucci, Scarlato, Harris, 2017; Tournigand et al., 2017) and an optical flow code (Sun et al., 2010a, 2010b) modified to generate "Tacho (velocity) Diagrams." The Rise Diagrams were used to calculate the initial jet velocity by determining the initial slope of the rising plume. Additionally, the Rise Diagrams were used to determine the peak plume height. We used the Watec camera to estimate plume height on occasions when the top of the plume exceeded the field of view of the infrared camera.

The optical flow method and resulting Tacho Diagrams are an extension of particle motion and particle image velocimetry algorithms (Mori & Chang, 2009), in which the algorithm determines the differences in two consecutive video-frames assigning velocity vectors to each pixel in the image (see Mori & Chang, 2009; Sun et al. 2010a, 2010b; and Text S1 for details).

Analysis of the Tacho Diagrams determines the velocity and flux timeseries of the plumes, as well as the peak jet velocity of the explosive event, the peak volume flux, and the cumulative volume of each event. The peak jet velocity is the maximum positive (vertical) velocity recorded during the explosive event (measured at the eleventh pixel line above the vent, i.e., ~26 m above Showa's crater rim, to avoid any edge effects). To account for outlier pixels, we used a 5 × 5 pixel median filter to smooth the image before determining the peak velocity. The volume flux uses the velocity timeseries multiplied by the maximum cross-sectional area of the plume (assuming circular geometry) to determine the volume of material passed by the reference line between frames (Text S1 and Figure S2). We assumed a constant plume width for the duration of each event, taken as the maximum width of the plume in the Tacho Diagram. This decision was made due to the sensitivity of the code to changing plume widths (within an order of magnitude) and the difficulty in consistently and accurately outlining the entire plume (See Figure S2c). The median value for measured plume widths was 65 m, which is reasonable when compared to the estimated vent radius of 45 m from Muramatsu et al. (2018). The peak volume flux was determined by taking the maximum flux value for the duration of the event. The cumulative plume volume is the sum of the fluxes calculated for each frame throughout the explosive event. The choice to use the maximum width of the explosive jet as a constant, and the assumption of circular plume throughout the eruption to calculate the cross-sectional area and corresponding flux and volume calculations, will likely provide upper (maximum) bounds on these values.

We analyzed data from two seismometers, each paired with a three-sensor infrasound array. Data from two Nanometrics Trillium Posthole Broadband 3-component seismometers and six InfraBSU infrasound sensors (range of ± 125 Pa) were recorded on a Nanometrics Centaur digitizer. A detailed description of the catalog creation for the full suite of seismic and infrasound events can be found in Smith et al. (2020). This study uses 97 complete explosive events (defined as having both seismic and infrasound data that matched with an infrared camera recording of the plume) (Text S2 and Table S2). Of these 97 events, 35 events had infrasound N-waves indicating potential shockwave development (Johnson et al., 2004; Mendez-Harper et al., 2018).

2.2. Measuring Electrical Activity

For this study, we used the lightning mapping array (LMA) system: an array of VHF sensors, which detects impulsive radio emissions from lightning, thus enabling the reconstruction of a four-dimensional "image" of the lightning flash or other electrical activity (Hamlin, 2004; Rison et al., 1999; Thomas et al., 2003, 2004). We used the LMA to measure different aspects of electrical activity within the plume, such as the timing of individual radio frequency (RF) sources, number of lightning flashes, and the presence of differing types of signals from electrical activity (Behnke et al., 2018). In this study we will use the following categories to define the electrical activity of a volcanic event: (a) the presence of vent discharges (was there a CRF signal during the eruption?), (b) the presence of lightning, and (c) the number of located RF sources—defined as the total number of electrical breakdown events that the lightning mapping array located during one

Table 1
Results of t-Tests

		Vent discharges (CRF)					Lightning				
Transform	Variable	*p*-value	Rank	Mean of No distribution[a] ($n = 73$)	Mean of yes distribution ($n = 24$)	Difference in means	*p*-values	Rank	Mean of No distribution ($n = 18$)	Mean of Yes distribution ($n = 79$)	Difference in means
$\log_{10}$	Initial jet top velocity	0.0002	***	27.89	53.43	25.54	0.0068	**	22.83	35.57	12.74
$\log_{10}$	Cumulative plume volume	0.0021	**	645,886.20	2,308,187.00	1,662,300.80	0.0141	*	453,417.20	1,030,863.00	577,445.80
$\log_{10}$	Peak volume flux	0.0027	**	30,064.85	135,216.60	105,151.75	0.0021	**	21,054.79	51,483.73	30,428.94
$1 / \sqrt{x}$	Peak jet velocity	0.0201	*	9.74	15.51	5.77	0.0554	.	8.74	11.41	2.66
–	Peak plume height	0.0283	*	834.12	1,015.50	181.38	0.5051	–	837.83	888.37	50.55

CRF, continual radio frequency.
[a]The Mean of Distribution columns are the mean value of the distribution for the selected variable made up of all events where there was or was not the CRF signal or lightning, respectively.
Note: – < 90%,. > 90%, *>95%, **>99%, ***>99.9% significance level.

explosive event. The number of located RF sources is a measure of the total amount of electrical activity (not broken down by discharge type) within the volcanic plume.

2.3. Statistical Analysis

We analyzed data from the five plume variables and categories of electrical activity using comparative *t*-tests to determine if there are any differences in plume parameters between events with a specific parameter and events without it. We used the Welch *t*-test to test the null hypothesis of equal means for samples of unequal variances.

Next, we combined plume parameters with seismic and infrasound data in a multivariable linear regression model to gain a more complete view of the eruption dynamics and how they relate to volcanic electrical activity (See Table S3 for all regression statistics). We used the geophysical variables from Equation 5 in Smith et al. (2020) reproduced here as Equation 1, including the seismic energy, infrasound energy, and duration of seismic signal:

$$\sqrt[2]{\mathrm{NLS}} = \beta_0 + \beta_{\mathrm{SE}}\left(\log_{10}\mathrm{SE}\right) + \beta_{\mathrm{IE}}\left(\log_{10}\mathrm{IE}\right) + \beta_{X2}\left(\log_{10}\mathrm{SE} * \log_{10}\mathrm{IE}\right) + \beta_{\mathrm{SD}}\sqrt[2]{\mathrm{SD}}, \quad (1)$$

where NLS is the number of located RF sources, SE is the seismic energy in Joules, IE is the infrasound energy in Joules, and SD is the seismic duration in seconds. We then followed the procedure for variable selection and model creation outlined in Smith et al. (2020) to determine the most significant variables for the best model for number of located RF sources with both plume and geophysical measurements.

3. Data and Results

3.1. Vent Discharges and Associated CRF Signals

We first examine the presence (or absence) of the CRF signal with relation to our derived plume parameters for all 97 explosive events. Table 1 shows the Welch's *t*-test results, indicating that there is a statistically significant difference (p-value < 0.05) between events with and without CRF signals for all five of the plume variables (See Table S4 for complementary Mann-Whitney *U*-test results). The explosions with vent discharges have statistically higher peak jet velocity, peak volume flux, peak plume height, initial jet top velocity, and cumulative plume volume. Production of vent discharges is statistically related to higher-velocity plumes with a higher flux of particles and gas.

3.2. Lightning

t-tests examining the presence or absence of lightning with respect to the five plume parameters showed that not all the plume parameters were significant. Explosive events with and without lightning were not statistically different for peak plume height ($p = 0.505$) and just marginally non-significantly different at the 95% level for peak jet velocity ($p = 0.055$). However, lightning production correlated to larger peak volume flux, higher initial jet top velocity, and larger cumulative volume of material released (99th%, 99th%, and 95th% confidence levels, respectively) (Table 1).

3.3. Plume and Geophysical Linear Model

The number of located RF sources is a measure of the total electrical activity in the plume, without distinguishing between vent discharges and lightning flashes. But, because vent discharges are distinguished by the CRF signal (that is, by definition, a large cluster of located RF sources over a longer period of time than a lightning flash), we can assume that events with many located RF sources are likely to contain vent discharges.

Our final multivariable linear regression model consisted of the following five variables: infrasound energy, seismic duration, peak volume flux, initial jet top velocity, and the peak plume height.

The final model equation is:

$$\log_{10}\mathrm{NLS} = \beta + \beta_{\mathrm{IE}} \log_{10}\mathrm{IE} + \beta_{\mathrm{SD}}\sqrt{\mathrm{SD}} + \beta_{\mathrm{PVF}} \log_{10}\mathrm{PVF} + \beta_{\mathrm{IJV}} \log_{10}\mathrm{IJV} + \beta_{\mathrm{PPH}}\mathrm{PPH}, \quad (2)$$

where: NLS, number of located RF sources; IE, infrasound energy; SD, seismic duration; PVF, peak volume flux; IJV, initial jet top velocity; and PPH, peak plume height.

The statistical effect plots (Figure 1) show positive correlations between each of these variables and the total number of located RF sources. Effect plots show the effect of each individual variable on the number of located RF sources while holding all other variables in the model constant. In this way, we can see how each individual variable contributes to the model. This model (Equation 2) has an adjusted R^2 of 0.52, compared to the R^2 of 0.35 from the model given by Equation 1. This indicates that the given set of variables explain just over half of the variation in the electrical activity of the plume, and that the addition of plume variables to the geophysical variables improves the model's explanation of NLS variation. The rest of the regression statistics for Equation 2 can be found in Text S3 and Table S5.

3.4. Threshold Values

Using the *t*-test results and the statistical model generated above we defined the following thresholds to differentiate explosive events with: (a) low to no volcanic electrical activity, (b) volcanic lightning only, and (c) volcanic lightning plus vent discharges (shown through the highest levels of electrical activity). These values are shown in the conceptual diagram in Figure 2 and duplicated in table form in Table S6. Threshold estimates for the plume parameters are based on the *t*-test values for the vent discharges and lightning. Threshold estimates for the seismic duration and infrasound energy were determined using Equation 2 and the predict function in R. We predict that 100 located RF sources (a large amount of electrical activity for this data set) that will occur at similar plume values as the volcanic lightning and vent discharges *t*-tests with the addition of infrasound energy greater than 10^7 J and seismic duration greater than 80 s. This infrasound energy estimate matches with the high electrical activity threshold value estimated by Smith et al. (2020).

4. Discussion

The results of our statistical model (Equation 2) confirm that the formation of a plume and its physical characteristics are important conditions for the production of volcanic electrical activity. This is intuitive because the generation of electrical discharges depends on the presence and separation of charge. The initial velocity of the top of the jet is an indication of the eruption rate, whereby higher rise velocities

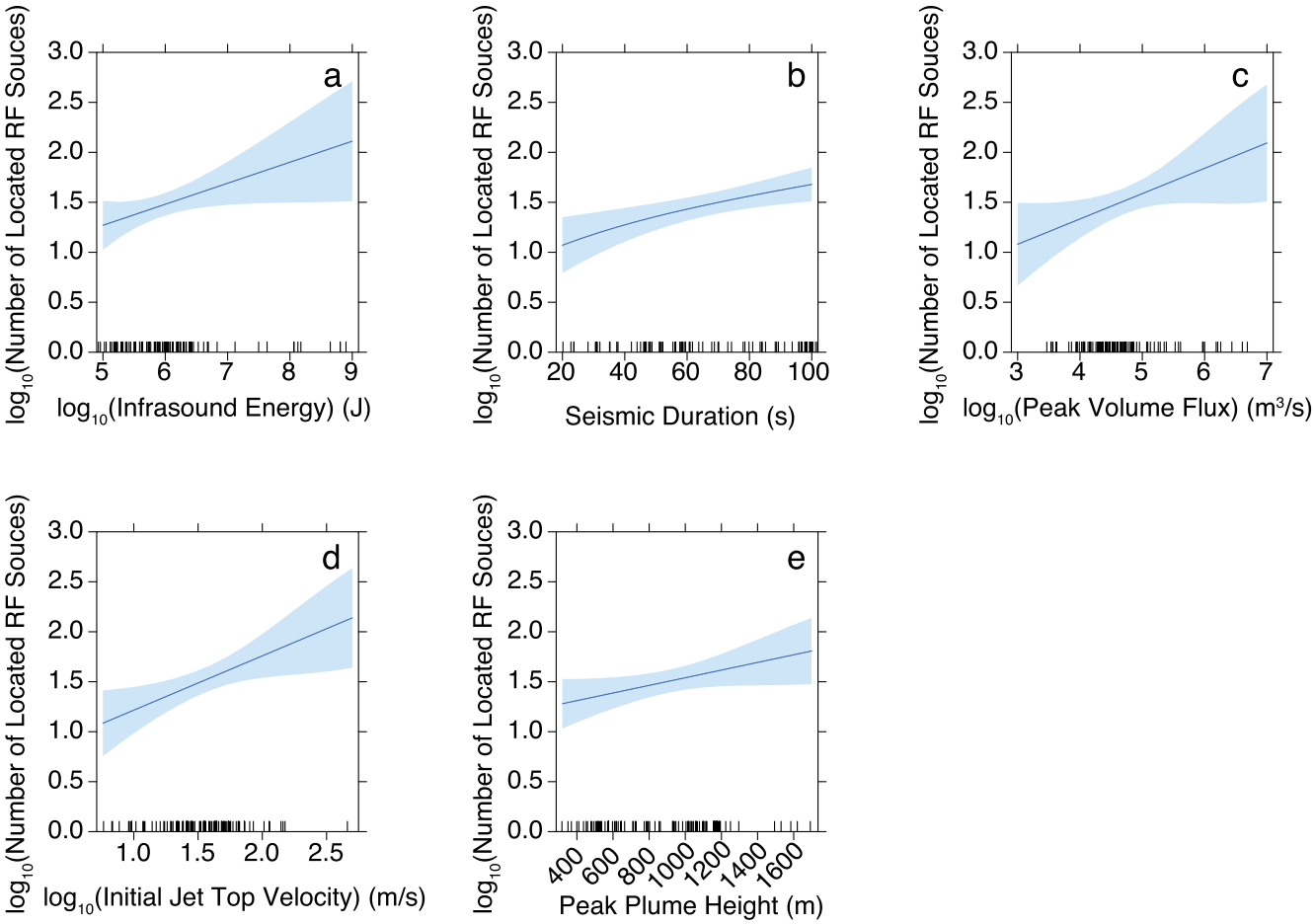

Figure 1. Statistical effect plots for the multivariable regression model of plume plus geophysical variables with respect to the number of located RF sources. Effect plots show the effect of varying the selected regressor variable on the response while holding all other regressors at their mean value. The tick marks along the *x*-axis of the plot show the distribution of samples. The light blue area surrounding the regression line indicates the 95% confidence interval of the model. (a) Effect plot for the infrasound energy. (b) Effect plot for the seismic duration. (c) Effect plot for the peak volume flux. (d) Effect plot for the initial jet top velocity. (e) Effect plot for the peak plume height.

would accompany explosions of higher intensity. Plumes rising faster are characterized by increased shear along the plume margins and higher turbulence, which in turn would enhance collisional charging of ash particles. Mareev and Dementyeva (2017) show that relative velocities and turbulence are key factors in noninductive and triboelectric charging. Additionally, rapidly expanding jets are more likely to generate shock waves, which have been shown by Méndez Harper et al. (2018) to enhance the conditions for electrical breakdown at the vent. The model results also imply that the production of volcanic electrical activity is related to the flux of material at the vent. More material exiting faster would result in more particle charging interactions, again creating favorable conditions for electrical discharge formation.

One key observation that comes from the *t*-tests is the difference in the mean values between events with and without vent discharges/lightning. From these, we infer that there is a spectrum for the generation of electrical activity generation within the period of observation at Sakurajima volcano. The smallest explosive events created no electrical activity, the mid-size events created volcanic lightning only, and the largest events created both vent discharges and lightning (Figure 2). Conceptually, this finding implies that to generate lightning there needs to be some amount of ash in the plume, but to generate CRF there needs to be both a large volume of ash and a strong, impulsive eruption. This corresponds to the potential relationship between shockwave occurrence and CRF generation, as suggested by the laboratory experiments of Mendez-Harper et al. (2018). This also corresponds to the previous study by Behnke et al. (2014) who showed that during the phreatomagmatic, highly explosive first stage of eruption at Eyjafjallajökull both lightning

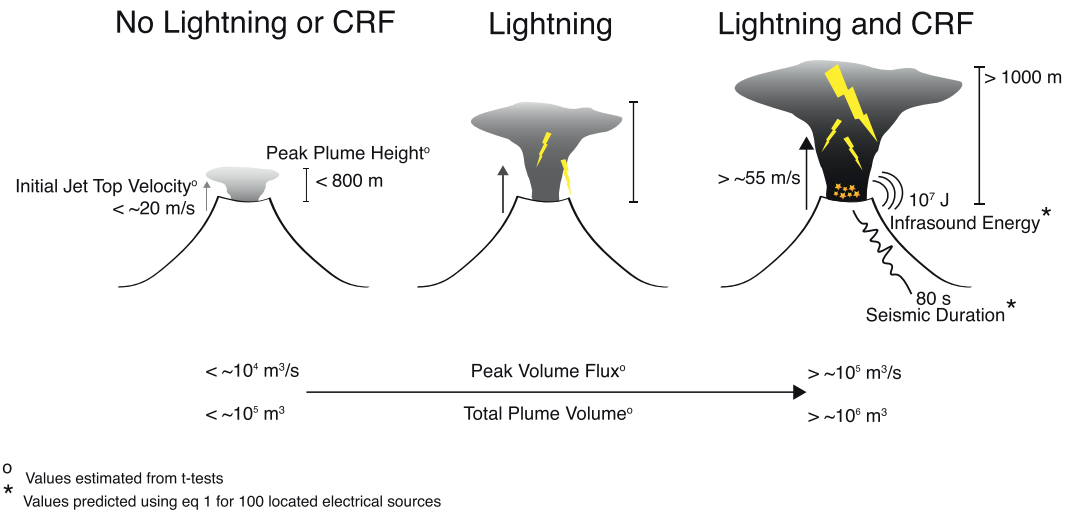

Figure 2. Conceptual model for when volcanic lightning and CRF will occur at Sakurajima volcano. Using the values from Table 1, Equation 1, and Table S5 to show the continuum from the smallest volcanic plumes recorded without either volcanic lightning or CRF, to mid-sized volcanic plumes (800–1,000 m) that had volcanic lightning (shown as the yellow lightning symbols) but no CRF signal, to the largest events observed during out study, which had both volcanic lightning and CRF (shown as the orange stars). CRF, continual radio frequency.

and CRF coexisted. However, in the less explosive second stage of the eruption only lightning was recorded by the LMA. This may be related to the amount fractoemission charging that occurs – more magma fragmentation will be expected to occur in stronger, more explosive eruptions. Experimental work has shown that the initial fragmentation of ash is an important charge generator in the vent region where CRF occurs (James et al., 2000; Mendez-Harper et al., 2015).

Although we cannot quantitatively differentiate between the proportion of solids and gas in the volume of the plume, the peak volume flux may be used as an indication of more charged material. If we make the simplifying assumption that the solid to gas proportion of the initial jet, before significant air entrainment, is constant, then the higher volume would mean more material injected into the plume. More charged material would allow for more electrical discharges to occur. Gaudin and Cimarelli (2019) showed, in lab-scale flows, that discharges cannot happen without ash. Based on observations of particle shape morphologies, Smith, Van Eaton, Charbonnier, et al. (2018) have shown that vent discharges, at Showa Crater, were more likely during explosions that resulted in the comminution of particles in the conduit. Thus, an increased volume flux suggests more ash forming (increasing fractoemission) and higher levels of ash interaction (increasing the potential for secondary fragmentation and triboelectrification) within the initial plume formation resulting in more electrical activity (shown here as the number of located RF sources).

The positive correlation between the peak plume height and the total electrical activity (Equation 1) may also indicate a relationship between the amount of material and eruption energy. The final plume height in unsteady Vulcanian eruptions relates to the buoyancy and momentum of the ejected material (Clarke et al., 2015). Additionally, the plumes in this dataset were all <3 km and therefore well below the −20°C isotherm required for ice charging to become a factor in electrical activity (Cimarelli et al., 2016; Durant et al., 2009; Van Eaton et al., 2020). Thus, this positive relationship is not linked to ice-charging phenomena, as seen in larger eruptions, but instead must relate to the hot material ejected into the atmosphere. Additionally, this positive correlation may be related to larger plumes having more effective charge separation between particles of different sizes.

The model (Equation 1) also shows the importance of the explosion source characteristics in generating volcanic electrical activity. Both infrasound energy and the duration of the seismic signal have positive correlations with the total number of located RF sources. These two parameters point to energetic explosions (high infrasound energy) that may occur at different depths within the conduit (long duration seismic

signals may result from extended decompression and fragmentation waves as they travel to deeper depths) (Clarke et al., 2015; Smith et al., 2020).

Limitations of this study include the small range of eruptions considered and the lack of information on the gas to ash ratio in the studied plumes. A study of this type will benefit from using a wide range of eruption sizes to develop the relationship between plume height and electrical activity. This relationship is important to understand as the height of the plume, along with ash concentration, plays the greatest role in determining aviation warnings.

5. Conclusions

The presence of lightning is most significantly related to the peak volume flux. This is an interesting parallel to meteorological thunderstorm studies which correlate updraft volumes with lightning flash rates. As the size of the eruption—measured through infrasound energy, seismic signal duration, peak volume flux, initial jet top velocity, and the peak height of the plume—increases, the electrical activity within the plume—measured by vent discharges, lightning flashes, and the number of located RF sources—will also increase. Our study reveals conditions under which volcanic lightning can occur without vent discharges (Figure 2), highlighting that vent discharges are not necessarily a precursor to volcanic lightning. In fact, vent discharges are not a lot of small lightning discharges but rather are small streamer discharges, which is one of the electrical breakdown processes that occurs in lightning (Behnke et al., 2018).

The value of volcanic lightning and vent discharges/CRF signals to hazard monitoring is due to the fact that they reveal that an ash-bearing plume has formed. This is unlike other geophysical signals. For example: seismic data may reflect the migration of magma within the volcano and associated deformations but it does not indicate if magma has breached the surface nor if ash has been erupted; infrasound data are often interpreted by the occurrence of an explosive event at the surface but does not help in distinguishing if this event was ash or gas rich; visual remote sensing methods like satellite need clear weather for visibility and are limited by overpass times and look angles. Alternatively, volcanic lightning is a clear indicator that (a) a plume is forming/has formed, (b) that there is ash in that plume, and (c) if the CRF signal is also present, that the eruption was large and impulsive. This is the first study to examine the minimum eruption size required to produce LMA-detected lightning and CRF signals. A better understanding of plume dynamics through lightning and CRF detection may lead to better modeling of the plumes and to better and more rapid civilian and aviation warnings in the long term. Using the electrical activity of the volcanic plume to monitor eruptions is not a way to replace any previous methods but rather a valid complementary source of information that can provide additional insight about the developing eruption cloud.

Data Availability Statement

All data are available in the supporting information, and raw instrument data are publicly available through the USF library digital collections at https://digital.lib.usf.edu/volcanic-lightning/

Acknowledgments
Funding support for this work was made possible by National Science Foundation Grants AGS 1445704 and 1445703 and NSF-EAR-PF 1855153. D. Gaudin and C. Cimarelli have been supported by the Marie Skłodowska-Curie Grant Agreement No. 705619. C. M. Smith and C. Cimarelli acknowledge the support of Deutsche Forschungsgemeinschaft project CI 254/2-1 to CC. Any use of trade, firm, or product names is for descriptive purposes only and does not imply endorsement by the U.S. Government. The authors would like to thank M. Iguchi, D. Miki, and all of the staff at the Sakurajima Volcano Observatory for their assistance during data collection. The authors would also like to thank John Lyons and two anonymous reviewers whose comments greatly improved this manuscript.

References

Aizawa, K., Cimarelli, C., Alatorre-Ibargüengoitia, M. A., Yokoo, A., Dingwell, D. B., & Iguchi, M. (2016). Physical properties of volcanic lightning: Constraints from magnetotelluric and video observations at Sakurajima volcano, Japan. *Earth and Planetary Science Letters*, *444*, 45–55. https://doi.org/10.1016/j.epsl.2016.03.024

Aizawa, K., Yokoo, A., Kanda, W., Ogawa, Y., & Iguchi, M. (2010). Magnetotelluric pulses generated by volcanic lightning at Sakurajima volcano, Japan. *Geophysical Research Letters*, *37*(17). https://doi.org/10.1029/2010GL044208

Arason, P., Petersen, G. N., & Bjornsson, H. (2013). *Estimation of eruption site location using volcanic lightning*. Icelandic Met Office Report VÍ, 6.

Behnke, S. A., Edens, H. E., Thomas, R. J., Smith, C. M., McNutt, S. R., Van Eaton, A. R., et al. (2018). Investigating the origin of continual radio frequency impulses during explosive volcanic eruptions. *Journal of Geophysical Research: Atmospheres*, *123*(8), 4157–4174. https://doi.org/10.1002/2017JD027990

Behnke, S. A., & McNutt, S. R. (2014). Using lightning observations as a volcanic eruption monitoring tool. *Bulletin of Volcanology*, *76*(8), 1–12. https://doi.org/10.1007/s00445-014-0847-1

Behnke, S. A., Thomas, R. J., Edens, H. E., Krehbiel, P. R., & Rison, W. (2014). The 2010 eruption of Eyjafjallajökull: Lightning and plume charge structure. *Journal of Geophysical Research: Atmospheres*, *119*(2), 833–859. https://doi.org/10.1002/2013JD020781

Behnke, S. A., Thomas, R. J., McNutt, S. R., Schneider, D. J., Krehbiel, P. R., Rison, W., & Edens, H. E. (2013). Observations of volcanic lightning during the 2009 eruption of Redoubt Volcano. *Journal of Volcanology and Geothermal Research*, *259*, 214–234. https://doi.org/10.1016/j.jvolgeores.2011.12.010

Calhoun, K. M., MacGorman, D. R., Ziegler, C. L., & Biggerstaff, M. I. (2013). Evolution of lightning activity and storm charge relative to dual-Doppler analysis of a high-precipitation supercell storm. *Monthly Weather Review*, *141*, 2199–2223. https://doi.org/10.1175/MWR-D-12-00258.1

Carey, L. D., Schultz, E. V., Schultz, C. J., Deierling, W., Petersen, W. A., Bain, A. L., & Pickering, K. E. (2019). An evaluation of relationships between radar-inferred kinematic and microphysical parameters and lightning flash rates in Alabama storms. *Atmosphere*, *10*, 796. https://doi.org/10.3390/atmos10120796

Cimarelli, C., Alatorre-Ibargüengoitia, M. A., Aizawa, K., Yokoo, A., Díaz-Marina, A., Iguchi, M., & Dingwell, D. B. (2016). Multiparametric observation of volcanic lightning: Sakurajima volcano, Japan. *Geophysical Research Letters*, *43*(9), 4221–4228. https://doi.org/10.1002/2015GL067445

Clarke, A. B., Esposti Ongaro, T., & Belousov, A. (2015). Vulcanian eruptions. In *The encyclopedia of volcanoes* (pp. 505–518, 2nd ed). Academic Press. https://doi.org/10.1016/B978-0-12-385938-9.00028-6

Deierling, W., & Petersen, W. A. (2008). Total lightning activity as an indicator of updraft characteristics. *Journal of Geophysical Research*, *113*, D16210. https://doi.org/10.1029/2007JD009598

Deierling, W., Petersen, W. A., Latham, J., Ellis, S., & Christian, H. J. (2008). The relationship between lightning activity and ice fluxes in thunderstorms. *Journal of Geophysical Research*, *113*, D15210. https://doi.org/10.1029/2007JD009700

Durant, A. J., Rose, W. I., Sarna-Wojcicki, A. M., Carey, S., & Volentik, A. C. M. (2009). Hydrometeor-enhanced tephra sedimentation: Constraints from the 18 May 1980 eruption of Mount St. Helens. *Journal of Geophysical Research*, *114*(B3), 1–21. https://doi.org/10.1029/2008JB005756

Gaudin, D., & Cimarelli, C. (2019). The electrification of volcanic jets and controlling parameters: A laboratory study. *Earth and Planetary Science Letters*, *513*, 69–80. https://doi.org/10.1016/j.epsl.2019.02.024

Gaudin, D., Taddeucci, J., Scarlato, P., del Bello, E., Ricci, T., Orr, T., et al. (2017). Integrating puffing and explosions in a general scheme for Strombolian-style activity. *Journal of Geophysical Research: Solid Earth*, *122*(3), 1860–1875. https://doi.org/10.1002/2016JB013707

Gaudin, D., Taddeucci, J., Scarlato, P., Harris, A., Bombrun, M., Del Bello, E., & Ricci, T. (2017). Characteristics of puffing activity revealed by ground-based, thermal infrared imaging: The example of Stromboli Volcano (Italy). *Bulletin of Volcanology*, *79*(3). https://doi.org/10.1007/s00445-017-1108-x

Hamlin, T. D. (2004). *The New Mexico Tech lightning mapping array*. New Mexico Institute of Mining and Technology.

James, M. R., Lane, S. J., & Gilbert, J. S. (2000). Volcanic plume electrification: Experimental investigation of a fracture-charging mechanism. *Journal of Geophysical Research*, *105*(B7), 16641–16649. https://doi.org/10.1029/2000JB900068

Johnson, J. B., Aster, R. C., & Kyle, P. R. (2004). Volcanic eruptions observed with infrasound. *Geophysical Research Letters*, *31*(L14604), 4. https://doi.org/10.1029/2004GL020020

Mareev, E. A., & Dementyeva, S. O. (2017). The role of turbulence in thunderstorm, snowstorm, and dust storm electrification. *Journal of Geophysical Research: Atmospheres*, *122*(13), 6976–6988. https://doi.org/10.1002/2016JD026150

Mather, T. A., & Harrison, R. G. (2006). Electrification of volcanic plumes. *Surveys in Geophysics*, *27*, 387–432. https://doi.org/10.1007/s10712-006-9007-2

McNutt, S. R., & Thomas, R. J. (2015). Volcanic Lightning. In *The encyclopedia of volcanoes* (pp. 1059–1067, 2nd ed). https://doi.org/10.1016/B978-0-12-385938-9.00062-6

McNutt, S. R., Thompson, G., West, M. E., Fee, D., Stihler, S., & Clark, E. (2013). Local seismic and infrasound observations of the 2009 explosive eruptions of Redoubt Volcano, Alaska. *Journal of Volcanology and Geothermal Research*, *259*, 63–76. https://doi.org/10.1016/j.jvolgeores.2013.03.016

McNutt, S. R., & Williams, E. R. (2010). Volcanic lightning: Global observations and constraints on source mechanisms. *Bulletin of Volcanology*, *72*(10), 1153–1167. https://doi.org/10.1007/s00445-010-0393-4

Méndez Harper, J., & Dufek, J. (2016). The effects of dynamics on the triboelectrification of volcanic ash. *Journal of Geophysical Research: Atmospheres*, *121*, 8209–8228. https://doi.org/10.1002/2015JD024663.Received10.1002/2015jd024275

Méndez Harper, J., Dufek, J., & Mcadams, J. (2015). The electrification of volcanic particles during the brittle fragmentation of the magma column. *Proceedings of ESA Annual Meeting on Electrostatics*, *10*.

Méndez Harper, J. S., Cimarelli, C., Dufek, J., Gaudin, D., & Thomas, R. J. (2018). Inferring compressible fluid dynamics from vent discharges during volcanic eruptions. *Geophysical Research Letters*, *45*(14), 7226–7235. https://doi.org/10.1029/2018GL078286

Mori, N., & Chang, K. (2009). *Introduction to MPIV: PIV toolbox in MATLAB*.

Muramatsu, D., Aizawa, K., Yokoo, A., Iguchi, M., & Tameguri, T. (2018). Estimation of Vent Radii from video recordings and infrasound data analysis: Implications for vulcanian eruptions from Sakurajima volcano, Japan. *Geophysical Research Letters*, *45*(23). https://doi.org/10.1029/2018GL079898

Prata, A. T., Folch, A., Prata, A. J., Biondi, R., Brenot, H., Cimarelli, C., et al. (2020). Anak Krakatau triggers volcanic freezer in the upper troposphere. *Scientific Reports*, *10*(1), 1–13. https://doi.org/10.1038/s41598-020-60465-w

Rison, W., Thomas, R. J., Krehbiel, P. R., Hamlin, T., & Harlin, J. (1999). A GPS-based three-dimensional lightning mapping system: Initial observations in central New Mexico. *Geophysical Research Letters*, *26*(23), 3573–3576. https://doi.org/10.1016/j.jval.2016.03.124510.1029/1999gl010856

Schultz, C. J., Carey, L. D., Schultz, E. V., & Blakeslee, R. J. (2017). Kinematic and microphysical significance of lightning jumps versus nonjump increases in total flash rate. *Weather and Forecasting*, *32*, 275–288. https://doi.org/10.1175/WAF-D-15-0175.1

Smith, C. M., Thompson, G., Reader, S., Behnke, S. A., McNutt, S. R., Thomas, R., & Edens, H. (2020). Examining the statistical relationships between volcanic seismic, infrasound, and electrical signals: A case study of Sakurajima volcano, 2015. *Journal of Volcanology and Geothermal Research*, *402*, 16996. https://doi.org/10.1016/j.jvolgeores.2020.106996

Smith, C. M., Van Eaton, A. R., Charbonnier, S., McNutt, S. R., Behnke, S. A., Thomas, R. J., et al. (2018). Correlating the electrification of volcanic plumes with ashfall textures at Sakurajima volcano, Japan. *Earth and Planetary Science Letters*, *492*, 47–58. https://doi.org/10.1016/j.epsl.2018.03.052

Smith, C. M., Van Eaton, A. R., Said, R., & Holzworth, R. H. (2018). Volcanic lightning as a monitoring tool during the 2016-2017 eruption of Bogoslof Volcano, AK. In *25th International Lightning Detect Conference & 7th International Lightning Meteorology Conference* (pp. 1–5).

Sun, D., Roth, S., & Black, M. J. (2010a). *A quantitative analysis of current practices in optical flow estimation and the principles behind them* (Technical Report Brown-CS-10-03). https://doi.org/10.1109/cvpr.2010.5539939

Sun, D., Roth, S., & Black, M. J. (2010b). Secrets of optical flow estimation and their principals. In *International Conference on Computer Vision & Pattern Recognition*. https://doi.org/10.1109/cvpr.2010.5539939

Thomas, R. J., Krehbiel, P. R., Rison, W., Harlin, J., Hamlin, T., & Campbell, N. (2003). The LMA flash algorithm. *Proceedings of the 12th International Conference on Atmospheric Electricity* (pp. 655–656). France: International Commission on Atmospheric Electricity Versailles.

Thomas, R. J., Krehbiel, P. R., Rison, W., Hunyady, S. J., Winn, W. P., Hamlin, T., & Harlin, J. (2004). Accuracy of the lightning mapping array. *Journal of Geophysical Research: Atmospheres*, *109*(14), 1–34. https://doi.org/10.1029/2004JD004549

Tournigand, P.-Y., Taddeucci, J., Gaudin, D., Peña Fernández, J. J., Del Bello, E., Scarlato, P., et al. (2017). The initial development of transient volcanic plumes as a function of source conditions. *Journal of Geophysical Research: Solid Earth*, *122*, 9784–9803. https://doi.org/10.1002/2017JB014907

Van Eaton, A. R., Amigo, Á., Bertin, D., Mastin, L. G., Giacosa, R. E., González, J., et al. (2016). Volcanic lightning and plume behavior reveal evolving hazards during the April 2015 eruption of Calbuco volcano, Chile. *Geophysical Research Letters*, *43*, 3563–3571. https://doi.org/10.1002/2016GL068076

Van Eaton, A. R., Schneider, D. J., Smith, C. M., Haney, M. M., Lyons, J. J., Said, R., et al. (2020). Did ice-charging generate volcanic lightning during the 2016–2017 eruption of Bogoslof volcano, Alaska? *Bulletin of Volcanology*, *82*(3), 24. https://doi.org/10.1007/s00445-019-1350-5

Williams, E. R., & McNutt, S. R. (2005). Total water contents in volcanic eruption clouds and implications for electrification and lightning. In C. Pontikis (Ed.), *Research signpost, recent progress in lightning physics* (p. 13). School of Geosciences Faculty and Staff Publications